The Impact of Rigidity and Water Exchange on the Relaxivity of a Dendritic MRI Contrast Agent

Gaëlle M. Nicolle,[a] Éva Tóth,[a] Heribert Schmitt-Willich,[b] Bernd Radüchel,[b] and André E. Merbach*[a]

Abstract: Variable-temperature, multiple magnetic field ^{17}O NMR, EPR and variable-temperature ^{1}H nuclear magnetic relaxation dispersion (NMRD) measurement techniques have been applied to Gadomer 17, a new dendritic contrast agent for magnetic resonance imaging. The macromolecule bears 24 Gd(dota)–monoamide chelates (dota = *N*,*N*′,*N*″,*N*‴-tetracarboxymethyl-1,4,7,10-tetraazacyclododecane) attached to a lysine-based dendrimer. ^{17}O NMR and ^{1}H NMRD data were analysed simultaneously by incorporating the Lipari–Szabó approach for the description of rotational dynamics. The water exchange rate k_{ex}^{298} was found to be $(1.0 \pm 0.1) \times 10^6\ s^{-1}$, a value similar to those measured for other Gd(dota)–monoamide complexes, and the activation parameters $\Delta H^{\neq} = 24.7 \pm 1.3$ kJ mol^{-1} and $\Delta S^{\neq} = -47.4 \pm 0.2$ J K^{-1} mol^{-1}. The internal flexibility of the macromolecule is characterised by the Lipari–Szabó order parameter $S^2 = 0.5$ and a local rotational correlation time $\tau_l^{298} =$ 760 ps, whereas the global rotational correlation time of the dendrimer is much longer, $\tau_g^{298} = 3050$ ps. The analysis of proton relaxivities reveals that, beside slow water exchange, internal flexibility is an important limiting factor for imaging magnetic fields. Electronic relaxation, though faster than in similar, but monomeric, Gd^{III} chelates, does not limit proton relaxivity of this contrast agent ($r_1 = 16.5$ mM^{-1} s^{-1} at 298 K and 20 MHz). This analysis provides direct clues for the design of high-efficiency contrast agents.

Keywords: dendrimers · gadolinium · imaging agents · Lipari–Szabó approach · magnetic resonance imaging · water exchange

Introduction

In the last two decades, magnetic resonance imaging (MRI) has become a powerful and widespread diagnostic technique in medicine, in part thanks to the use of Gd^{III}-based contrast agents. The improvement of the signal-to-noise ratio of the image obtained in the presence of a contrast agent is correlated to the proton relaxivity, r_1, of the agent. The relaxivity is defined as the enhancement of the relaxation rate of water protons in the presence of the paramagnetic compound compared with that in pure water, referred to a 1 mM concentration of Gd^{III}. Despite the high performance of MRI, there is a constant need to improve the accuracy of the technique, as well as its specificity towards different organs and tissues. With the aim of judiciously increasing the proton relaxivity of contrast agents, a new generation of Gd^{III} complexes has been developed based on macromolecular assemblies (polymers, micelles, protein-bound complexes).[1–8] Beside the relaxivity gain originating from the increased molecular size, these macromolecular agents also allow the blood pool to be targeted, thanks to reduced extravasation after intravenous administration (magnetic resonance angiography).[9–10] Gd^{III} chelates attached to dendrimers have already proved to fulfil the requirements of blood-pool agents. In addition, dendrimers are monodisperse and can be synthesised in a controllable manner, both factors representing an advantage over other polymeric contrast agents.[11–14]

Some years ago, the first ^{17}O NMR study of Gd^{III}-based polyamidoamine (PAMAM) dendrimers opened the way to the understanding of the parameters that play a crucial role in the efficacy of such contrast agents.[6] Recently, a novel, pharmacokinetically more useful dendritic Gd^{III} complex, Gadomer 17, has been proposed, mainly for the visualisation of the vascular anatomy.[14] Gadomer 17 is based on a trimesoyl triamide central core to which 18 lysine amino acid residues are attached, binding 24 Gd(dota)–monoamide complexes (dota = *N*,*N*′,*N*″,*N*‴-tetracarboxymethyl-1,4,7,10-tetraazacyclododecane) on the surface of the dendrimer, as shown in the formula and in Figure 1.[15] The Gd^{III} complex is

[a] Prof. A. E. Merbach, G. M. Nicolle, Dr. É. Tóth
Institut de Chimie Moléculaire et Biologique
EPFL-BCH
1015 Lausanne (Switzerland)
Fax: (+41) 21-693-98-75
E-mail: andre.merbach@epfl.ch

[b] Dr. H. Schmitt-Willich, Dr. B. Radüchel
Schering AG, Berlin (Germany)

Supporting information for this article is available on the WWW under http://www.wiley-vch.de/home/chemistry/ or from the author.

0947-6539/02/0805-1040 $ 17.50+.50/0 *Chem. Eur. J.* **2002**, *8*, No. 5

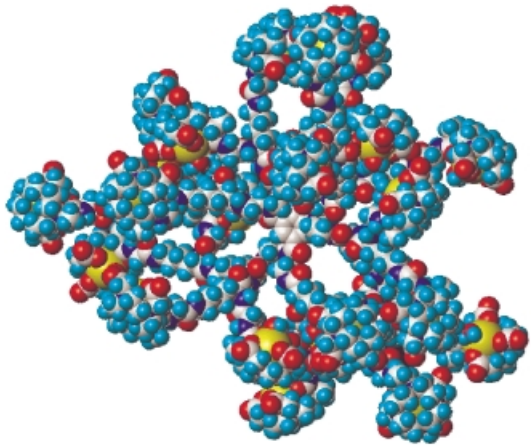

Figure 1. Structure of Gadomer 17 obtained by molecular modelling.

neutral to ensure low osmolality. Here we report on the structural and dynamic parameters governing the relaxivity of Gadomer 17, determined from variable-temperature and multiple magnetic field EPR, ^{17}O NMR and variable-temperature ^{1}H NMRD studies. For the first time for dendrimer complexes, the rotational dynamics has been treated with the Lipari–Szabó approach. This analysis allows the separation of global and local motion, and gives direct information about the rigidity of the macromolecule.[16–17] It is well known that internal flexibility accounts for the limited proton relaxivity gain for many macromolecular Gd^{III} complexes, therefore it is very important to separate the contributions of global and local rotational motion to the overall relaxivity. As a consequence of the special structure of Gadomer 17, some of the Gd^{III} centres are situated relatively close to each other. The short Gd–Gd distance may result in significant increases of the electron spin relaxation rates, owing to dipole–dipole interactions between Gd spins.[18–19] The accelerated electronic relaxation may then become a limiting factor for proton relaxivity; this would consequently put a serious limit on increasing the number of Gd^{III} ions in a small space in the case of macromolecular MRI contrast agents. These crucial and novel aspects have been addressed in this study.

Results

UV/Vis spectroscopy: The $^{7}F_0 - {}^{5}D_0$ transition band of Eu^{III} in the range 577.5–581.5 nm is very sensitive to the coordination environment and is often used to test for the presence of differently coordinated or hydrated species in solution.[1, 20] The Eu^{III} analogue of Gadomer 17 has a single, temperature-invariant absorption band in this region, which proves there is no hydration equilibrium in solution. Moreover, the position of the peak, compared with literature data, allows assignment of the band to the monohydrated Eu^{III} complex.[21] By analogy, we can assume that the same monohydrated species also exists for the corresponding Gd^{III} complex.

^{17}O NMR and NMRD spectroscopy: We have measured variable-temperature ^{17}O relaxation rates and chemical shifts at two magnetic fields (1.41 and 9.4 T), proton relaxivities as a function of the Larmor frequency at five different temperatures, and variable-temperature transverse electron spin relaxation rates at three magnetic fields for aqueous solutions of Gadomer 17. None of the ^{17}O-reduced relaxation rates and chemical shifts, $1/T_{1r}$, $1/T_{2r}$ and $\Delta\omega_r$, nor the proton relaxivities, r_1, nor the transverse electronic relaxation rates, $1/T_{2e}$, showed concentration dependence; therefore data measured at different concentrations (Table 1) have been fitted together. Recently, for many Gd^{III} complexes, experimental data from ^{17}O NMR, EPR and NMRD spectroscopy have been analysed simultaneously. This approach is based on the numerous common parameters of these three techniques and has the advantage of determining more reliably the set of parameters that determine proton relaxivity. Unfortunately, a simultaneous analysis of all EPR, ^{17}O and NMRD data was unsuccessful for Gadomer 17. All attempts clearly showed

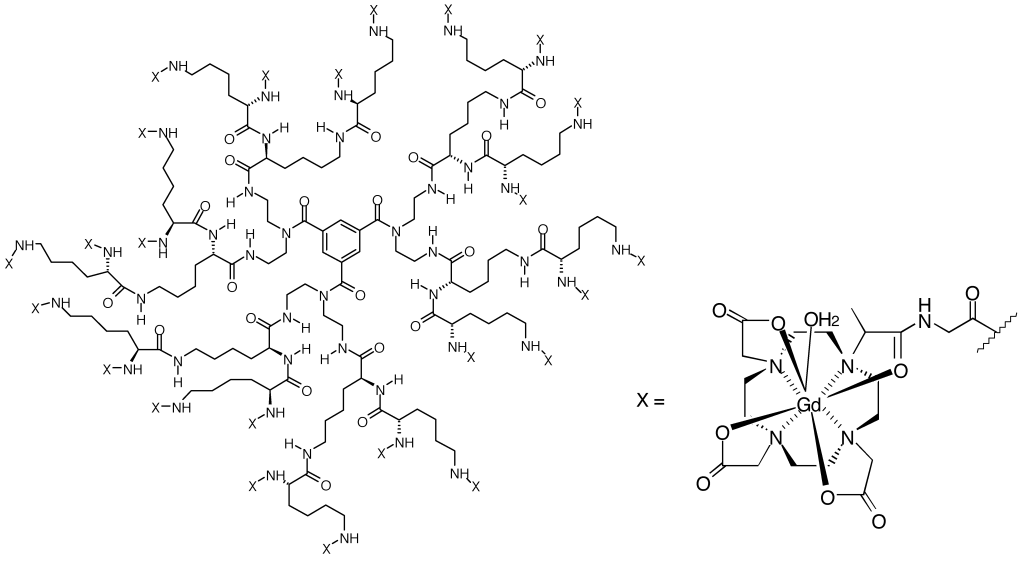

Gadomer 17

  0947-6539/02/0805-1041 $ 17.50+.50/0

Table 1. Composition of the different solutions used in this work.

Method	Solution	$[Gd^{3+}]$ [mmol kg^{-1}]	pH
EPR X-band	Gadomer 17	40.6	5.92
EPR 150 and 225 GHz	Gadomer 17	45.3	5.80
EPR 150 and 225 GHz	Gadomer 17	92.8	6.03
^{17}O NMR 9.4 T	Gadomer 17	17.8	6.17
^{17}O NMR 1.41 and 9.4 T	Gadomer 17	70.9	5.78
^{17}O NMR 1.41 and 9.4 T	Water reference	–	4.20
^{1}H NMRD	Gadomer 17	5.2	5.85

that this failure is due to the incompatibility of the electronic relaxation parameters as determined by the three different techniques. The experimental data gathered by EPR, ^{17}O NMR and NMRD spectroscopy cover a large magnetic field range; this further complicates the analysis. Previous studies, including those of macromolecular systems, have already revealed the lack of an appropriate theory of electron spin relaxation in Gd^{III} complexes to describe the field dependence as well as the relation between longitudinal and transverse relaxation rates (only the latter is accessible experimentally by EPR spectroscopy). Substantial improvement has been achieved with the recent theoretical developments by Borel, Rast et al.[22–23] However, their theory is not applicable to macromolecular Gd^{III} complexes for which the Redfield limit is not respected. In fact, one assumption is that the energy of the spin–lattice coupling is smaller than the inverse of the correlation time, and thus the inverse of the rotation correlation time, which is not valid for large molecules. Therefore, given the lack of an adequate theoretical approach, we could only analyse ^{17}O NMR and NMRD data together, and fit the variable-field EPR data separately.

The transverse ^{17}O relaxation rate of the bound water, T_{2m}, has been expressed by a simple exponential law versus the inverse temperature as in previous studies, including dendrimer complexes.[6, 24] The analysis of $1/T_{2m}$ in terms of a scalar relaxation mechanism,[25] which is governed by water exchange and electronic relaxation, impeded the fitting, undoubtedly because of the incomplete description of the electronic relaxation. In the analysis of the longitudinal ^{17}O relaxation rates, we have used the Lipari–Szabó approach. The proton relaxivities have been treated with the usual Solomon–Bloembergen–Morgan equations, combined with the Lipari–Szabó approach for the description of the rotational dynamics (see below and Appendix). This procedure, in which the ^{17}O $1/T_{2m}$ is treated in a simplified manner, implies that the electronic relaxation parameters (the correlation time of the zero-field splitting (ZFS), τ_v, and the mean square of the ZFS energy, Δ^2) are only determined by NMRD spectroscopy. They should, therefore, be considered more as fitting parameters and one should not attribute too much physical meaning to them.

The longitudinal ^{17}O relaxation rates, presented in Figure 2b, depend on the magnetic field, an observation that always indicates slow rotation. The Solomon–Bloembergen spectral density functions for non-extreme-narrowing conditions could not appropriately describe the experimental data. As previously for other macromolecular systems,[2, 26] we applied the spectral density functions of the Lipari–Szabó

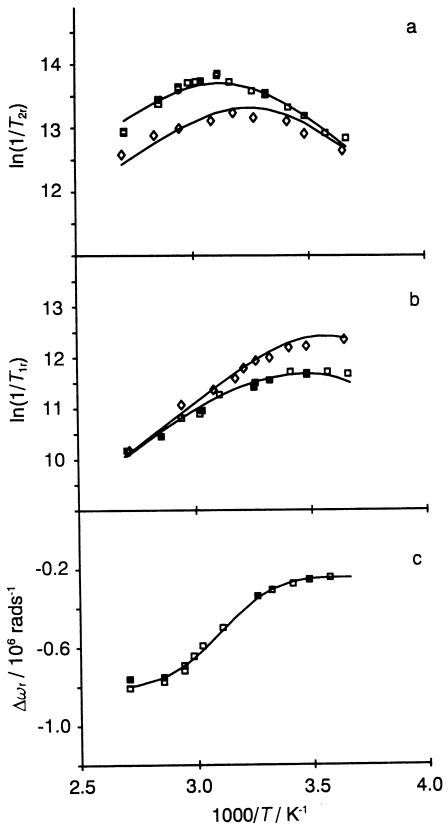

Figure 2. Temperature dependence of the reduced ^{17}O transverse (a) and longitudinal (b) relaxation rates, and of the reduced chemical shifts (c). B = 1.41 T (◇) or 9.4 T (□ and ■); c_{Gd} = 70.9 mM (□ and ◇) and c_{Gd} = 17.8 mM (■).

model for the analysis of both ^{17}O and ^{1}H longitudinal relaxation data. This model has been already used to analyse nuclear magnetic resonance relaxation data in terms of rotational dynamics for solutions of proteins,[27–28] peptides,[29] sugars,[30–31] micellised surfactants[32] and calixarenes.[33] In this approach, the modulation of the interaction causing the relaxation is considered as the result of two statistically independent motions; a rapid local motion, which is in the extreme narrowing conditions, with a correlation time τ_l, and a slower global motion of the whole molecule with a correlation time τ_g. The model also provides a general order parameter, $\mathcal{S}^2$, which describes the degree of spatial restriction of the local motion: if the internal motion is fully isotropic, $\mathcal{S}^2 = 0$; if the rotational dynamics is governed exclusively by the global motion, $\mathcal{S}^2 = 1$.

The ^{17}O NMR and ^{1}H NMRD experimental data as well as the fitted curves are presented in Figures 2 and 3, respectively, and the resulting kinetic and NMR parameters are given in Table 2. All relevant equations used in the analysis are listed in the Appendix. The diffusion constant, D^{298}_{GdH}, obtained in the fit is $(18 \pm 1) \times 10^{-10}$ m^2 s^{-1}; its activation energy, E_{GdH}, was fixed to the common value of 20 kJ mol^{-1}.[18] The distances used in the analysis were fixed as the following usual values: the effective distance between the Gd^{III} electron spin and the ^{17}O nucleus r_{GdO} = 2.5 Å, that between the electron spin and the ^{1}H nucleus r_{GdH} = 3.1 Å, and the closest approach of the bulk water molecules a_{GdH} = 3.5 Å: for the quadrupolar coupling constant we obtained $\chi(1+\eta^2/3)^{1/2} = 5.5 \pm 0.6$ MHz.

0947-6539/02/0805-1042 $ 17.50+.50/0 Chem. Eur. J. 2002, 8, No. 5

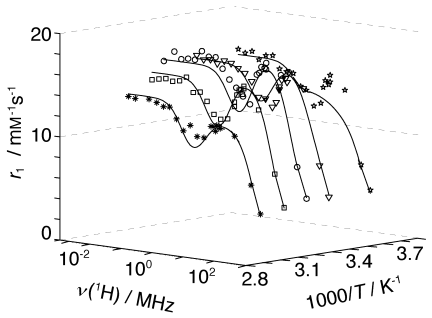

Figure 3. Three-dimensional representation of NMRD profiles of Gadomer 17 at 5 °C (☆), 25 °C (▽), 37 °C (○), 50 °C (□) and 65 °C (✳), c_{Gd} = 5.2 mM.

Table 2. Kinetic and NMR parameters obtained from the simultaneous fit of ^{17}O NMR and ^1H NMRD data.

Gd^{III} complexes	[Gd(DO3A-bz-NO_2)(H_2O)][a]	G_3Gd_{23}[b]	Gadomer 17[c]
k_{ex}^{298} [$\times 10^6$ s^{-1}]	1.6	1.0	1.0 ± 0.1
$\Delta H^{\neq}$ [kJ mol^{-1}]	40.9	28.8	24.7 ± 1.3
$\Delta S^{\neq}$ [J mol^{-1} K^{-1}]	+11.1	−30	-47.4 ± 0.2
$A/\hbar$ [$\times 10^6$ rad s^{-1}]	−3.8	−3.9	-3.8 ± 0.1
c_{os}	0.06	0.11	0.26 ± 0.08
τ_R^{298} [ps]	210	580	τ_g^{298} 3050 ± 250
			τ_l^{298} 760 ± 120
E_R [kJ mol^{-1}]	17.7	23.6	E_g 28 ± 2
			E_l 52 ± 6
$\mathcal{S}^2$		–	0.50 ± 0.02
τ_v^{298} [ps]		–	46 ± 3
E_v [kJ mol^{-1}]		–	1.0[d]
Δ^2 [10^{20} s^{-2}]		–	0.070 ± 0.004

[a] From reference [6]. [b] PAMAM dendrimer of generation 3 with 23 Gd^{III}(DO3A)–monoamide chelates.[6] [c] Lysine-based dendrimer with 24 Gd^{III}(dota)–monoamide chelates (see formula and Figure 1). [d] This parameter was fixed for the fit.

The transverse ^{17}O relaxation rates obtained for the bound water molecule are $1/T_{2m}^{298,LF} = (1.5 \pm 0.2) \times 10^6\ s^{-1}$ ($B = 1.41$ T) and $1/T_{2m}^{298,HF} = (2.6 \pm 0.1) \times 10^6\ s^{-1}$ ($B = 9.4$ T) with an associated activation energy $E_m = 22.1 \pm 0.2$ kJ mol^{-1}.

EPR spectroscopy: The EPR lines appeared at a field corresponding to the Landé factor g_L (equal to 2.0 taking experimental error into consideration), and had approximately a Lorentzian shape. The experimental electron spin relaxation rates at all frequencies (9.4, 150, 225 GHz) are markedly higher than those measured on small molecular weight Gd^{III} complexes with a similar chelating unit.[18] This indicates that, beside the transient zero-field splitting mechanism,[34–35] one has to assume another contribution. Previous EPR studies on dimer[18] or trimer[19] Gd^{III} complexes have already indicated that intramolecular dipole–dipole interactions may operate between the close Gd^{III} ions, resulting in an increase of the transverse electron spin relaxation rate. Molecular dynamics simulations—though they were performed only for a vacuum—show that some Gd–Gd distances, r_{GdGd}, in Gadomer 17 are as short as 5.8 Å (see Figure 1).[36] This distance is much less than those in the previously studied dimers, [bisoxa{Gd(DO3A)(H_2O)}$_2$] and [pip{Gd(DO3A)(H_2O)}$_2$], in which $r_{GdGd} = 9.3$ Å and 8.7 Å, respectively, where the contribution from intramolecular interaction is not negligible (DO3A = 1,4,7,10-tetraazacyclododecane-1,4,7-tris(acetic acid)). This contribution was more relevant at high magnetic fields and was probably modulated by molecular reorientation.[18] Therefore, we propose that the high transverse electron spin relaxation rates observed for Gadomer 17 in EPR spectra can also be accounted for by intramolecular Gd–Gd interactions. The experimental $1/T_{2e}$ values were thus treated as the sum of zero-field splitting and intramolecular dipole–dipole contributions. We supposed that the intramolecular interaction is modulated by the global rotational motion of the dendrimer; thus, the correlation time for this mechanism, τ_{Re}, has been fixed at the value of the global rotational correlation time previously obtained from the analysis of ^{17}O and ^1H longitudinal relaxation rates. Hence, the analysis of the variable-temperature, multiple-field EPR data resulted in parameters describing the zero-field splitting relaxation mechanism (τ_v and Δ^2) as well as in an effective Gd–Gd distance. In principle, there are a large number of Gd–Gd distances (24×23) to be taken into account in such an analysis, which is hardly practicable. Consequently, the single effective distance that we obtain can be related to the average value of all available Gd–Gd distances in Gadomer 17. However, one has to be aware of the deficiency of such an evaluation of the EPR data. Given the lack of a reliable theory of electron spin relaxation for macromolecular Gd^{III} systems, this analysis can only point out in a qualitative way that an intramolecular dipole–dipole mechanism also contributes to the overall electronic relaxation. The temperature dependence of the transverse electronic relaxation rates as well as the fitted curves are shown in Figure 4.

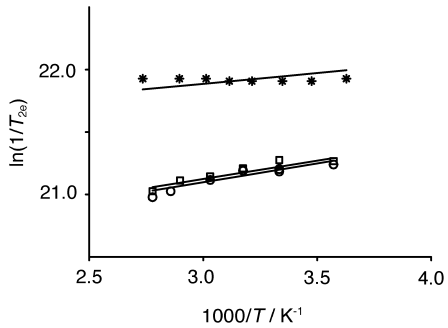

Figure 4. Temperature dependence of the transverse electronic relaxation rates of Gadomer 17 at $B = 0.34$ T (✳)($c_{Gd} = 40.6$ mM; pH = 5.9), 5.4 T (□) and 8.1 T (○) (at both high fields $c_{Gd} = 45.3$ mM and 92.8 mM). The parameters obtained in the fit are $\tau_v^{298} = 16.4 \pm 2.5$ ps, $\Delta^2 = 0.16 \pm 0.01 \times 10^{20}$ s^{-2}, $r_{GdGd} = 12.6 \pm 0.1$ Å, $E_{Re} = 2.7 \pm 0.3$ kJ mol^{-1}, with E_v and τ_{Re}^{298} fixed to 1.0 kJ mol^{-1} and 3050 ps.

Discussion

Water exchange kinetics: The water exchange rate is a critical issue for macromolecular Gd^{III} chelates as potential MRI contrast agents, since low exchange rates often limit proton relaxivity.[6] The k_{ex} value obtained for Gadomer 17 is very similar to those found for structurally similar, dota–monoamide derivatives such as [Gd(DO3A-bz-NO_2)(H_2O)] (Table 2). This is in accordance with previous observations

showing that structural differences outside the inner coordination sphere do not influence the rate and mechanism of water exchange on the gadolinium centre.[1] The hyperfine coupling constant $A/\hbar$, which is a measure of the electron delocalisation from the metal ion onto the ligand nucleus, has the usual value found for Gd^{III} complexes (Table 2). This fact indicates that the assumption of one inner-sphere water molecule is correct; further support comes from the UV/Vis measurements on the Eu^{III} analogue (see above).

Rotational dynamics: Analysis of the longitudinal ^{17}O relaxation rates has only been possible by means of the Lipari–Szabó approach;[16–17] this is an indication of the slow rotation of this dendrimer. The large difference between the local and global rotational correlation times (τ_l and τ_g) shows that the motion of a given Gd^{III} chelate attached to the dendrimer, characterised by τ_l, is considerably faster than that of the whole macromolecule (τ_g). This, plus the value of the order parameter, $\mathcal{S}^2 = 0.5$, are clear indications of the internal flexibility of the dendrimer. (It has to be noted that the order parameter is sufficiently high to be accurately determined.[16–17]) Compared with the linear Gd(dtpa-ba)–alkyl copolymers (dtpa = diethylenetriaminepentaacetic acid, ba = bisamide), [{Gd(dtpa-ba)–$(CH_2)_n$}$_x$] ($n = 10$, 12), this dendrimer is somewhat less flexible, as demonstrated by its higher $\mathcal{S}^2$ value ($\mathcal{S}^2 = 0.5$ for Gadomer 17; $\mathcal{S}^2 = 0.35$ for [{Gd(dtpa-ba)–$(CH_2)_n$}$_x$]; see Table 3). As stated by Lipari and Szabó, the generalised order parameter, $\mathcal{S}^2$, cannot be uniquely interpreted and its value can be consistent with an infinite number of physical pictures of the motion.[17] However, one can assume simple models and interpret $\mathcal{S}^2$ within the framework of the model chosen, an approach especially useful in relating similar systems. A simple model, which makes sense physically for both the dendrimer and linear polymer complex, assumes that the orientation vector of the internal motion diffuses within a cone of semiangle θ_0. For such a model, $\mathcal{S}$ can be related to the cone semiangle: $\mathcal{S}_{cone} = \frac{1}{2}(\cos\theta_0)(1+\cos\theta_0)$;[17] from this we obtain $\theta_0 = 45.8^\circ$ and 37.8° for the linear polymer and Gadomer 17, respectively.

Table 3. Comparison of rotational dynamics parameters for a linear copolymer and the studied dendrimer.

	[{Gd(dtpa-ba)–$(CH_2)_{12}$}$_n$][a]	Gadomer 17
Weight average [kDa]	15.7	17.5
τ_g^{298} [ps]	4400	3050 ± 250
τ_g^{298} [ps]	480	760 ± 120
E_g [kJ mol^{-1}]	23.3	28 ± 2
E_l [kJ mol^{-1}]	34.6	52 ± 6
$\mathcal{S}^2$	0.35	0.50 ± 0.02

[a] From reference [26].

The parameters obtained by the Lipari–Szabó approach to the rotational dynamics of the linear polymers [{Gd(dtpa-ba)–$(CH_2)_x$}$_n$] ($x = 10$, 12) could well explain the difference in proton relaxivity between the two polymers of different chain length.[26] It is more difficult to make a direct comparison between those polymers and the dendrimeric system studied here. On the basis of only the higher rigidity and faster water exchange rate of Gadomer 17, this dendrimer should have higher proton relaxivities than the linear polymer [{Gd(dtpa-ba)–$(CH_2)_{12}$}$_n$]. However, other factors, mainly the global rotational correlation time, which is shorter for Gadomer 17, cut back the relaxivity gain.

Electronic relaxation: The transverse electronic relaxation rates are much higher than previously observed for similar but monomeric Gd^{III} chelates. This difference has been interpreted as the result of an additional intramolecular dipole–dipole relaxation mechanism, which contributes 40% of the total transverse relaxation rate at 20 MHz, according to the parameters calculated from the variable-field EPR data. In this analysis, we obtained an effective Gd–Gd distance of $r_{Gd-Gd} = 12.6$ Å, which is similar to the arithmetical mean value (weighted by $1/r^6$) of all Gd–Gd distances determined from the molecular dynamics calculations (in vacuum, $r_{Gd-Gd} = 13.5$ Å).[36] This similarity also seems to support the conjecture of an intramolecular dipole–dipole relaxation mechanism operating in this system. Unfortunately, we could not incorporate this electron spin relaxation mechanism into the analysis of the ^{17}O NMR and NMRD data, probably because of the lack of an appropriate theory to describe the zero-field splitting relaxation mechanism for macromolecular Gd^{III} complexes.

It should be noted that the problems associated with electron spin relaxation have practically no effect on the determination of the parameters characterising water exchange and rotation. The presence of a well-defined slow exchange region in the ^{17}O $1/T_{2r}$ curves (Figure 2a) ensures the correct determination of the water exchange rate, whereas the longitudinal ^{17}O relaxation rates that are used together with the ^1H NMRD data for the calculation of the rotational parameters are hardly influenced by electronic relaxation. In the NMRD profiles, rotational parameters are mainly determined by the high-field values, where the effect of electronic relaxation is negligible.

Implications for proton relaxivity: The high-field peak observed around 30 MHz on the NMRD profiles of Gadomer 17, which is characteristic of slowly rotating chelates, has a maximum as a function of temperature. The reason for this behaviour is that at low temperatures the relaxivity is mainly limited by slow water exchange, whereas at high temperatures it is fast rotation that limits r_1. The Lipari–Szabó analysis of the rotational dynamics clearly shows that there is considerable internal flexibility, and this will cut back the relaxivity gain at imaging fields (20–60 MHz). The simulations in Figure 5 illustrate it well: when the rigidity, as quantified by the Lipari–Szabó order parameter $\mathcal{S}^2$, is increased, the relaxivity markedly increases (by a factor of 2 between $\mathcal{S}^2 = 0.5$, representing the actual case, and $\mathcal{S}^2 = 1$ which would be an ideal, rigid system), provided the water exchange rate is optimised. One can take full advantage of very long global rotational correlation times only if the macromolecule has high rigidity. Another important point is that higher imaging fields are not beneficial from the relaxivity point of view.

0947-6539/02/0805-1044 $ 17.50+.50/0 *Chem. Eur. J.* **2002**, *8*, No. 5

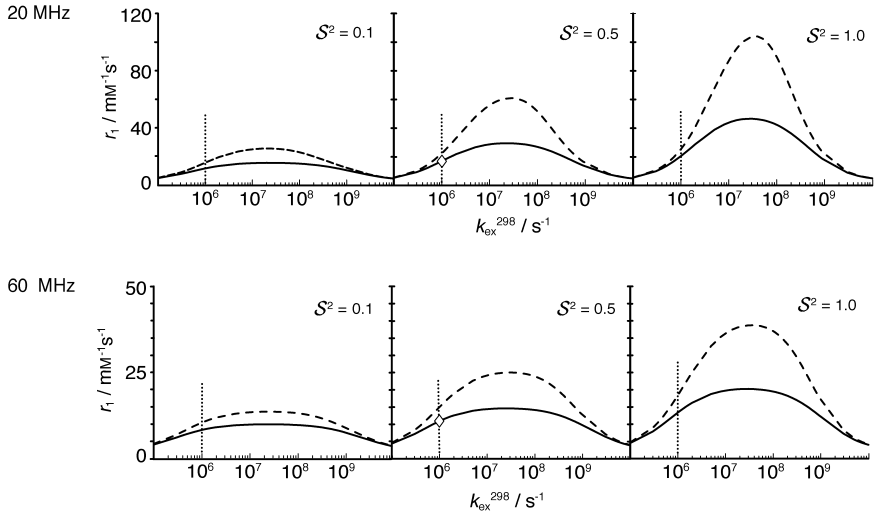

Figure 5. Simulated proton relaxivities as a function of the water exchange rate, k_{ex}, for different values of the global rotational correlation time, τ_g^{298}, and of the general order parameter, $\mathcal{S}^2$. $T = 37.0\,^{\circ}C$, $B = 0.47$ T (20 MHz) and 1.41 T (60 MHz). $\tau_g^{298} = 30$ ns and 3 ns for dotted and straight lines, respectively; $\tau_I^{298} = 0.76$ ns. $\diamond$ corresponds to the actual relaxivity of Gadomer 17.

Moreover, as these simulations show, the water exchange rate is also an important limiting factor for macromolecular compounds.[37] The maximum relaxivity on the simulated curves is reached around $k_{ex}^{298} = 34 \times 10^6\ s^{-1}$. With such an optimal water exchange rate, the relaxivity gain could be enormous for a large and rigid macromolecular system.

Since the electron spin relaxation in Gadomer 17, as measured directly by EPR spectroscopy, is faster than in similar, monomeric chelates, we wanted to check if this increased relaxation rate also constitutes a limiting factor for proton relaxivity. Figure 6 shows simulated relaxivities as a

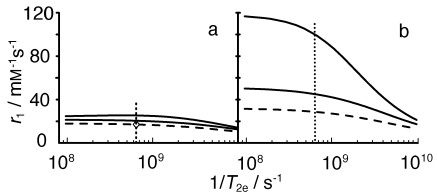

Figure 6. Simulated proton relaxivities as a function of the transverse electron spin relaxation rate, T_{2e}, for different values of the global rotational correlation time, τ_g^{298}, and of the water exchange rate: a) $k_{ex}^{298} = 1 \times 10^6\ s^{-1}$; b) $k_{ex}^{298} = 34 \times 10^6\ s^{-1}$. $T = 37.0\,^{\circ}C$, $B = 0.47$ T (20 MHz). From top down: $\tau_g^{298} = 30$ and 3 ns; $\mathcal{S}^2 = 1.0$. The dotted lines were simulated with the rotational parameters of Gadomer 17: $\mathcal{S}^2 = 0.5$, $\tau_g^{298} = 3$ ns, $\tau_I^{298} = 0.76$ ns. $\diamond$ corresponds to the actual relaxivity of Gadomer 17.

function of the transverse electron spin relaxation rate for the actual water exchange rate on Gadomer 17 and for an optimal k_{ex} value, as well as for different values of the rotational correlation time. Clearly, even the increased electron spin relaxation rate has no limiting effect for the relaxivity of Gadomer 17; such a limitation could be important only at optimal water exchange rates and rotational correlation times.

In conclusion, both slow water exchange and fast rotation, owing to the flexibility of the dendrimer, limit the proton relaxivity of Gadomer 17. Electron spin relaxation, regardless of its nature, is not a limiting factor for the proton relaxivity of this dendrimeric contrast agent.

Experimental Section

Synthesis of Gadomer 17: The monomeric macrocyclic ligand was prepared by monoalkylation of 1,4,7,10-tetraazacyclododecane (cyclen) with rac-*N*-(2-bromopropionyl)-glycine benzyl ester followed by exhaustive *N*-alkylation with *tert*-butyl bromoacetate. The benzyl ester was removed by hydrogenation and the resulting *tert*-butyl-protected ligand with the free glycine carboxylic acid in the side chain was converted into the *p*-nitrophenyl ester by conventional carbodiimide activation. Separately, the dendritic backbone was prepared as the fully benzyloxycarbonyl-protected 24mer amine. First the building block *N,N′*-(iminodi-2,1-ethandiyl)-bis{*N*2,*N*6-bis[(benzyloxy)carbonyl]-L-lysinamide} was prepared in a single step from commercially available starting materials. Three equivalents of this small dendron were then reacted with the central core benzene-1,3,5-tricarbonyl trichloride to give the benzyloxycarbonyl-protected 12mer amine in 80% yield. This precursor was easily converted to the free 12mer amine by means of HBr in acetic acid, and the 12 free amino groups that resulted were subsequently treated with N_α,N_ε-dibenzyloxycarbonyl-L-lysine-*p*-nitrophenyl ester to give the fully protected 24mer amine in >80% yield after chromatography (CH_2Cl_2/methanol 18/2). This compound shows the desired molecular peak at 6015 Da ([M^++Na]) by MALDI-TOF mass spectrometry. Finally, the protected 24mer amine was converted into the free 24mer amine by standard methods (HBr/acetic acid). Coupling of a threefold molar excess (72 mol per mol polyamine) of the *p*-nitrophenyl ester of the macrocyclic dota derivative described above was performed in dimethylformamide. Subsequently, the *tert*-butyl protecting groups were cleaved (trifluoroacetic acid) and an ultrafiltration (YM 3 AMICON, cut off 3000 Da) was performed. Complexation of the dendritic ligand with Gd_2O_3 at 80 °C in water yielded Gadomer 17 in 85% yield based on the polyamine backbone. This compound was fully characterised by analytical methods and shows the expected molecular peak at 17453 Da by MALDI-TOF mass spectrometry. A more detailed description of the synthesis has been given previously.[38]

Sample preparation: All solutions were prepared by dissolving a weighed amount of the complex in twice-distilled water. The pH (5.8–6.2) was adjusted by addition of known amounts of sodium hydroxide or perchloric acid solutions (Merck, p.a. 70%). The absence of free Gd^{III} ions was checked by the xylenol orange test.[39] The solutions for ^{17}O NMR measurements were enriched to 1% for the reference (water acidified with perchloric acid) and 2% for the solutions of Gadomer 17, using 10% ^{17}O-enriched water (Yeda, Rehovot, Israel). The compositions of the different solutions are given in Table 1.

For all measurements, the temperature was fixed with a gas flow and checked by a substitution method.[40]

UV/Vis spectroscopy: The absorption spectra of the Eu^{III} analogue of Gadomer 17 were recorded at two different temperatures, 24.8 and 48.5 °C, on a Perkin–Elmer Lambda 19 spectrometer. The measurements were carried out in cells equipped with thermostats with a 1 cm optical path length $\lambda = 577.5 - 581.5$ nm ($c_{Eu^{III}} = 53.16$ mM and pH = 6.2).

EPR spectroscopy: The X-band spectra (9.42 GHz, 0.34 T) were recorded on a Bruker ESP 300E spectrometer in continuous wave mode. The samples were sealed in 1 mm glass tubes. The peak-to-peak linewidths were measured directly from the recorded spectra. The measurements at high fields (150 GHz, 5.4 T; 225 GHz, 8.1 T) were performed on a home-built spectrometer (Technical University of Budapest). A quartz-stabilised

Gunn diode oscillator (Radiometer Physics) generated a microwave source at 75 MHz, which was then amplified by a frequency multiplier. The peak-to-peak linewidths were measured for three different concentrations, listed in Table 1. The temperature was stabilised with an Oxford Instruments ITC 502 control unit.

^{17}O NMR spectroscopy: Transverse and longitudinal ^{17}O relaxation rates and chemical shifts were measured for temperatures between 273 and 373 K. The Gd^{III} concentration independence was checked for two concentrations, given in Table 1. The data were recorded on a Bruker AMX 400 spectrometer (9.4 T; 54.2 MHz), and on a PW-60 electromagnet connected to a Bruker AC-200 console (1.41 T; 60 MHz). The samples were sealed in glass spheres adapted for 10 mm NMR tubes to avoid susceptibility corrections of the chemical shifts.[41] Bruker VT-1000 and VT 2000 temperature-control units were used to maintain constant temperature. The longitudinal and transverse relaxation times, T_1 and T_2, were obtained with the inversion–recovery[42] and the Carr–Purcell–Meiboom–Gill[43] spin echo techniques, respectively.

^{1}H NMRD spectroscopy: The longitudinal ^{1}H relaxation rates were measured at five temperatures from 278.15 to 348.15 K. The measurements were performed on a Spinmaster FFC (fast field cycling) NMR relaxometer equipped with a VTC90 temperature control unit (Stelar, Italy) (7×10^{-4}–0.47 T; 0.01–20 MHz) or on different Bruker spectrometers: an AC200 console connected to a WP-60 electromagnet, equipped with a home-built tunable probehead (0.66–1.41 T; 28–60 MHz), an AMX200 (4.7 T; 200 MHz) and DPX400 (9.4 T; 400 MHz). The samples were sealed in capillary tubes for the measurements between 28 and 60 MHz and in cylindrical tubes at all other frequencies.

Data analysis: The least-squares fit of the data was performed by a program working on a Matlab platform, version 5.3.[44–45]

Appendix

EPR spectroscopy: The transverse electronic relaxation rates, $1/T_{2e}$, were directly calculated from the measured peak-to-peak EPR linewidths, ΔH_{pp}, according to Equation (1), where μ_B is the Bohr magneton and h the Planck constant.[46]

$$\frac{1}{T_{2e}} = \frac{g_L \mu_B \pi \sqrt{3}}{h} \Delta Hpp \tag{1}$$

This transverse electronic relaxation rate has been described as the sum of two contributions, the zero-field splitting (ZFS), which generally dominates the electronic relaxation process, and the intramolecular interaction. The transient zero-field splitting mechanism exists for electrons with $S > 1/2$ in anisotropic lattices and is correlated with distortion in the structure of the complex. The longitudinal and transverse electronic relaxation rates $(1/T_{1e})^{ZFS}$ and $(1/T_{2e})^{ZFS}$ are expressed in Equations (2) and (3), where τ_v is the electronic correlation time for the modulation of the zero-field-splitting interaction, E_v the activation energy, Δ^2 the mean square zero-field-splitting energy and ω_S the Larmor frequency of the Gd^{III} electron spin.[34–35] We assume that τ_v obeys a simple exponential dependence on $1/T$ [Eq. (4)].

$$\left(\frac{1}{T_{1e}}\right)^{ZFS} = \frac{1}{25}\Delta^2\tau_v\{4S(S+1)-3\}\left(\frac{1}{1+\omega_S^2\tau_v^2}+\frac{4}{1+4\omega_S^2\tau_v^2}\right) \tag{2}$$

$$\left(\frac{1}{T_{2e}}\right)^{ZFS} = \Delta^2\tau_v\left(\frac{5.26}{1+0.372\omega_S^2\tau_v^2}+\frac{7.18}{1+1.24\omega_S\tau_v}\right) \tag{3}$$

$$\tau_v = \tau_v^{298}\left\{\frac{E_v}{R}\left(\frac{1}{T}-\frac{1}{298.15}\right)\right\} \tag{4}$$

The electronic relaxation rates due to the intramolecular Gd–Gd interaction and the corresponding spectral density function are given in Equations (5) and (6).[47]

$$\left(\frac{1}{T_{2e}}\right)^{intra} = \frac{1}{5}\left(\frac{\mu_0}{4\pi}\right)^2 \frac{\hbar^2\gamma_S^4 S(S+1)}{r_{GdGd}^6}\{3J_0^{intra}+5J_1^{intra}+J_2^{intra}\} \tag{5}$$

$$J_n^{intra} = \frac{\tau_{Re}}{1+n^2\omega_S^2\tau_{Re}^2} \qquad n = 0, 1, 2 \tag{6}$$

Lipari–Szabó approach to the rotational dynamics: The Lipari–Szabó spectral density functions are expressed in Equations (7)–(12), in which ω_I is the proton resonance frequency at the applied magnetic field and ω_S is the Larmor frequency of the electron spin, as before. Several equations in the following sections use these functions.

$$J(\omega_I;\tau_{d1}) = \left(\frac{\mathcal{S}^2\tau_{d1g}}{1+\omega_I^2\tau_{d1g}^2}+\frac{(1-\mathcal{S}^2)\tau_{d1}}{1+\omega_I^2\tau_{d1}^2}\right) \tag{7}$$

$$J(\omega_S;\tau_{d2}) = \left(\frac{\mathcal{S}^2\tau_{d2g}}{1+\omega_S^2\tau_{d2g}^2}+\frac{(1-\mathcal{S}^2)\tau_{d2}}{1+\omega_S^2\tau_{d2}^2}\right) \tag{8}$$

$$J_i(\omega_I) = \left(\frac{\mathcal{S}^2\tau_g}{1+i^2\omega_I^2\tau_g^2}+\frac{(1-\mathcal{S}^2)\tau}{1+i^2\omega_I^2\tau^2}\right) \qquad i = 1, 2 \tag{9}$$

$$\frac{1}{\tau_{dig}} = \frac{1}{\tau_m}+\frac{1}{\tau_g}+\frac{1}{T_{ie}} \qquad i = 1, 2 \tag{10}$$

$$\frac{1}{\tau_{di}} = \frac{1}{\tau_m}+\frac{1}{\tau}+\frac{1}{T_{ie}} \qquad i = 1, 2 \tag{11}$$

$$\frac{1}{\tau} = \frac{1}{\tau_g}+\frac{1}{\tau_l} \qquad i = 1, 2 \tag{12}$$

^{17}O NMR spectroscopy: The ^{17}O NMR measurements provide the relaxation rates and angular frequencies of the paramagnetic solutions, $1/T_1$, $1/T_2$ and ω, and of the acidified water reference, $1/T_{1A}$, $1/T_{2A}$ and ω_A. This allows the calculation of the reduced relaxation rates and chemical shift, $1/T_{1r}$, $1/T_{2r}$ and $\Delta\omega_r$, according to Equations (13)–(15). The parameters $1/T_{1m}$ and $1/T_{2m}$ are the relaxation rates of the bound water and $\Delta\omega_m$ is the chemical shift difference between bound and bulk water. The term τ_m is the mean residence time or the inverse of the water exchange rate, k_{ex}, and P_m is the mole fraction of the bound water.[48–49]

$$\frac{1}{T_{1r}} = \frac{1}{P_m}\left[\frac{1}{T_1}-\frac{1}{T_{1A}}\right] = \frac{1}{T_1+\tau_m}+\frac{1}{T_{1os}} \tag{13}$$

$$\frac{1}{T_{2r}} = \frac{1}{P_m}\left[\frac{1}{T_2}-\frac{1}{T_{2A}}\right] = \frac{1}{\tau_m}\frac{T_{2m}^{-2}+\tau_m^{-1}T_{2m}^{-1}+\Delta\omega_m^2}{(\tau_m^{-1}+T_{2m}^{-1})^2+\Delta\omega_m^2}+\frac{1}{T_{2os}} \tag{14}$$

$$\Delta\omega_r = \frac{1}{P_m}(\omega-\omega_A) = \frac{\Delta\omega_m}{(1+\tau_m T_{2m}^{-1})^2+\tau_m^2\Delta\omega_m^2}+\Delta\omega_{os} \tag{15}$$

Outer-sphere contributions to ^{17}O relaxation can be neglected.[25] Equations (13) and (14) can thus be further simplified to give Equations (16) and (17).

$$\frac{1}{T_{1r}} = \frac{1}{T_{1m}+\tau_m} \tag{16}$$

$$\frac{1}{T_{2r}} = \frac{1}{T_{2m}+\tau_m} \tag{17}$$

The temperature dependence of the water exchange rate is described by the Eyring equation [Eq. (18)], where ΔS^+ and ΔH^+ are the entropy and enthalpy of activation for the water exchange process, and k_{ex}^{298} is the water exchange rate at 298.15 K.

$$\frac{1}{T_m} = k_{ex} = \frac{k_B T}{h}\exp\left\{\frac{\Delta S^+}{R}-\frac{\Delta H^+}{RT}\right\} = \frac{k_{ex}^{298}T}{298.15}\exp\left\{\frac{\Delta H^+}{R}\left(\frac{1}{298.15}-\frac{1}{T}\right)\right\} \tag{18}$$

The transverse relaxation rate of the bound water, T_{2m}, is described by Equation (19), where E_m is the activation energy and $1/T_{2m}^{298,HF}$, $1/T_{2m}^{298,LF}$ are the transverse relaxation rates of the bound water at 9.4 T and 1.41 T, respectively, and at 298.15 K.

$$\frac{1}{T_{2m}} = \frac{1}{T_{2m}^{298,HF/LF}}\exp\left\{\frac{E_m}{R}\left(\frac{1}{T}-\frac{1}{298.15}\right)\right\} \tag{19}$$

The ^{17}O longitudinal relaxation rates for Gd^{III} solutions are the sum of dipolar and quadrupolar (in the approximation developed by Halle) contributions, expressed by Equations (20)–(22), where γ_S and γ_I are the electron and nuclear gyromagnetic ratios, respectively ($\gamma_S = 1.76 \times$

0947-6539/02/0805-1046 $ 17.50+.50/0 *Chem. Eur. J.* **2002**, *8*, No. 5

10^{11} rad s^{-1} T^{-1}, $\gamma_I = -3.626 \times 10^7$ rad s^{-1} T^{-1}), r_{GdO} is the effective distance between the electron charge and the ^{17}O nucleus, I is the nuclear spin (5/2 for ^{17}O), χ is the quadrupolar coupling constant and η is an asymmetry parameter.

$$\frac{1}{T_{1m}} = \frac{1}{T_{1dd}} + \frac{1}{T_{1q}} \tag{20}$$

$$\frac{1}{T_{1dd}} = \frac{2}{15}\left(\frac{\mu_0}{4\pi}\right)^2 \frac{\hbar^2\gamma_I^2\gamma_S^2}{r_{GdO}^6} S(S+1) \times [3J(\omega_I;\tau_{d1}) + 7J(\omega_S;\tau_{d2})] \tag{21}$$

$$\frac{1}{T_{1q}} = \frac{3\pi^2}{10}\frac{2I+3}{I^2(2I-1)}\chi^2(1+\eta^2/3) \times [0.2J_1(\omega_I) + 0.8J_2(\omega_I)] \tag{22}$$

The chemical shift of the bound water molecule, $\Delta\omega_m$, depends on the hyperfine interaction between the Gd^{III} electron spin and the ^{17}O nucleus and is directly proportional to the scalar coupling constant, $A/\hbar$, as expressed in Equation (23).[50]

$$\Delta\omega_m = \frac{g_L\mu_B S(S+1)B}{3k_B T}\frac{A}{\hbar} \tag{23}$$

The isotopic Landé g factor is equal to 2.0 for Gd^{III}, B represents the magnetic field, and k_B is the usual Boltzmann constant.

The outer-sphere contribution to the ^{17}O chemical shifts is proportional to $\Delta\omega_m$, as expressed in Equation (24), where C_{os} is an empirical constant.[25, 51]

$$\Delta\omega_{os} = C_{os}\Delta\omega_m \tag{24}$$

^{1}H NMRD: The measured longitudinal proton relaxation rate, R_1^{obs}, is the sum of a paramagnetic and a diamagnetic contribution [Eq. (25)], where r_1 represents the proton relaxivity.

$$R_1^{obs} = R_1^d + R_1^p = R_1^d + r_1[Gd^{3+}] \tag{25}$$

The term r_1 can be decomposed into inner-sphere and outer-sphere contributions as demonstrated in Equation (26); the expression of the inner-sphere term is given in Equation (27), where q is the number of inner-sphere water molecules.[48, 52]

$$r_1 = r_{1is} + r_{1os} \tag{26}$$

$$r_{1is} = \frac{1}{1000} \times \frac{q}{55.55} \times \frac{1}{T_{1m}^H + \tau_m} \tag{27}$$

The longitudinal relaxation rate of the inner-sphere protons, $1/T_{1m}^H$, is expressed by Equation (28), where r_{GdH} is the effective distance between the electron charge and the ^{1}H nucleus. The outer-sphere contribution can be described by Equation (29), where N_A is the Avogadro constant, a_{GdH} the closest approach distance of the water molecule and the complex, D_{GdH} is the sum of the diffusion of the water and the complex, and τ_{GdH} is a diffusional correlation time such as $\tau_{GdH} = a_{GdH}^2/D_{GdH}$. The associated spectral density function, J_{os}, is given in Equation (30).[53–54]

$$\frac{1}{T_{1m}^H} = \frac{2}{15}\left(\frac{\mu_0}{4\pi}\right)^2 \frac{\hbar^2\gamma_I^2\gamma_S^2}{r_{GdH}^6} S(S+1) \times [3J(\omega_I;\tau_{d1}) + 7J(\omega_S;\tau_{d2})] \tag{28}$$

$$r_{1os} = \frac{32N_A\pi}{405}\left(\frac{\mu_0}{4\pi}\right)^2 \frac{\hbar^2\gamma_S^2\gamma_I^2}{a_{GdH}D_{GdH}} S(S+1)\,[3J_{os}(\omega_I;T_{1e}) + 7J_{os}(\omega_S;T_{2e})] \tag{29}$$

$$J_{os}(\omega;T_{je}) = Re\left[\frac{1 + \frac{1}{4}\left(i\omega\tau_{GdH} + \frac{\tau_{GdH}}{T_{j_e}}\right)^{\frac{1}{2}}}{1 + \left(i\omega\tau_{GdH} + \frac{\tau_{GdH}}{T_{j_e}}\right)^{\frac{1}{2}} + \frac{4}{9}\left(i\omega\tau_{GdH} + \frac{\tau_{GdH}}{T_{j_e}}\right) + \frac{1}{9}\left(i\omega\tau_{GdH} + \frac{\tau_{GdH}}{T_{j_e}}\right)^{\frac{3}{2}}}\right] \qquad j = 1, 2 \tag{30}$$

The diffusion coefficient, D_{GdH}, is assumed to obey an exponential law versus $1/T$, with an activation energy E_{GdH}, as in Equation (31), in which D_{GdH}^{298} is the diffusion coefficient at 298.15 K.

$$D_{GdH} = D_{GdH}^{298}\,\exp\left\{\frac{E_{D_{GdH}}}{R}\left(\frac{1}{T} - \frac{1}{298.15}\right)\right\} \tag{31}$$

Acknowledgements

We thank Lothar Helm and Frank Dunand for the helpful discussions. We are grateful to Prof. András Jánossy, László Burai and Ferenc Simon for the high-field EPR measurements performed in Budapest. We thank Detlev Sülzle (Schering AG, Berlin), for the molecular modelling calculations. This work was supported by the Swiss National Science Foundation and within the EU COST Action D18.

[1] *The Chemistry of Contrast Agents in Medical Magnetic Resonance Imaging* (Eds.: A. E. Merbach, E. Tóth), Wiley, **2001**, p. 68.
[2] F. A. Dunand, E. Tóth, R. Hollister, A. E. Merbach, *J. Biol. Inorg. Chem.* **2001**, *6*, 247.
[3] J. P. André, E. Tóth, H. Fischer, A. Seelig, H. R. Mäcke, A. E. Merbach, *Chem. Eur. J.* **1999**, *5*, 2977.
[4] E. Tóth, F. Connac, L. Helm, K. Adzamli, A. E. Merbach, *J. Biol. Inorg. Chem.* **1998**, *3*, 606.
[5] K. E. Kellar, P. M. Henrichs, R. Hollister, S. H. Koenig, J. Eck, D. Wei, *Magn. Reson. Med.* **1997**, *38*, 712.
[6] E. Tóth, D. Pubanz, S. Vauthey, L. Helm, A. E. Merbach, *Chem. Eur. J.* **1996**, *2*, 1607.
[7] S. Aime, M. Botta, M. Fasano, S. G. Crich, E. Terreno, *J. Biol. Inorg. Chem.* **1996**, *1*, 312.
[8] E. C. Wiener, M. W. Brechbiel, H. Brothers, R. L. Magi, O. A. Gansow, D. A. Tomalia, P. C. Lauterbur, *Magn. Reson. Med.* **1994**, *31*, 1.
[9] L. J. M. Kroft, A. de Roos, *J. Magn. Reson. Imaging* **1999**, *10*, 395.
[10] R. C. Brasch, *Magn. Reson. Med.* **1991**, *22*, 282.
[11] J. W. M. Bulte, C. Wu, M. W. Brechbiel, R. A. Brooks, J. Vymazal, M. Holla, J. A. Frank, *Invest. Radiol.* **1998**, *33*, 841.
[12] M. Fischer, F. Vögtle, *Angew. Chem.* **1999**, *111*, 934; *Angew. Chem. Int. Ed.* **1999**, *38*, 884.
[13] D. K. Smith, F. Diederich, *Chem. Eur. J.* **1998**, *4*, 1353.
[14] Q. Dong, D. R. Hurst, H. J. Weinmann, T. L. Chenevert, F. J. Londy, M. R. Prince, *Invest. Radiol.* **1998**, *33*, 699.
[15] B. Raduechel, H. Schmitt-Willich, J. Platzek, W. Ebert, T. Frenzel, B. Misselwitz, H. J. Weinmann, *Book of Abstracts, 216th ACS National Meeting, PPMSE-278*, Boston, **1998**.
[16] G. Lipari, A. Szabó, *J. Am. Chem. Soc.* **1982**, *104*, 4546.
[17] G. Lipari, A. Szabó, *J. Am. Chem. Soc.* **1982**, *104*, 4559.
[18] D. H. Powell, O. M. Ni Dhubhghaill, D. Pubanz, Y. Lebedev, W. Schlaepfer, A. E. Merbach, *J. Am. Chem. Soc.* **1996**, *118*, 9333.
[19] E. Tóth, L. Helm, A. E. Merbach, R. Hedinger, K. Hegetschweiler, A. Jánossy, *Inorg. Chem.* **1998**, *37*, 4104.
[20] N. Graeppi, D. H. Powell, G. Laurenczy, L. Zekany, A. E. Merbach, *Inorg. Chim. Acta* **1995**, *235*, 311.
[21] S. T. Frey, W. De W. Horrocks, Jr., *Inorg. Chim. Acta*, **1995**, *229*, 383.
[22] S. Rast, A. Borel, L. Helm, E. Belorizky, P. H. Fries, A. E. Merbach, *J. Am. Chem. Soc.* **2001**, *123*, 2637.
[23] S. Rast, P. H. Fries, E. Belorizky, A. Borel, L. Helm, A. E. Merbach, *J. Chem. Phys.* **2001**, *115*, 7554.
[24] É. Tóth, S. Vauthey, D. Pubanz, A. E. Merbach, *Inorg. Chem.* **1996**, *35*, 3375.
[25] K. Micskei, L. Helm, E. Brücher, A. E. Merbach, *Inorg. Chem.* **1993**, *32*, 3844.
[26] E. Tóth, L. Helm, K. E. Kellar, A. E. Merbach, *Chem. Eur. J.* **1999**, *5*, 1202.
[27] M. D. Kemple, P. Buckley, P. Yuan, F. G. Prendergast, *Biochem.* **1997**, *36*, 1678.
[28] P. Tsan, J. C. Hus, M. Caffrey, D. Marion, M. Blackledge, *J. Am. Chem. Soc.* **2000**, *122*, 5603.
[29] K. H. Mayo, V. A. Daragan, D. Idiyatullin, I. Nesmelova, *J. Magn. Reson.* **2000**, *146*, 188.
[30] L. Maler, G. Widmalm, J. Kowalewski, *J. Phys. Chem.* **1996**, *100*, 17103.
[31] M. Effemey, J. Lang, J. Kowalewski, *Magn. Reson. Chem.* **2000**, *38*, 1012.
[32] K. Elbayed, D. Canet, J. Brondeau, *Mol. Phys.* **1989**, *68*, 295.
[33] J. H. Antony, A. Dölle, T. Fliege, A. Geiger, *J. Phys. Chem.* **1997**, *101*, 4517.

[34] A. D. McLachlan, *Proc. R. Soc. London* **1964**, *280*, 271.
[35] D. H. Powell, A. E. Merbach, G. González, E. Brücher, K. Micskei, M. F. Ottaviani, K. Köhler, A. von Zelewsky, O. Y. Grinberg, Y. Lebedev, *Helv. Chim. Acta* **1993**, *76*, 1.
[36] D. Sülzle (Schering AG, Berlin), private communication.
[37] D. M. J. Doble, M. Botta, J. Wang, S. Aime, A. Barge, K. N. Raymond, *J. Am. Chem. Soc.* **2001**, *123*, 10758.
[38] Schering AG, USP 5820849, **1996** example 1a–k.
[39] G. Brunisholz, M. Randin, *Helv. Chim. Acta* **1959**, *42*, 1927.
[40] C. Ammann, P. Meier, A. E. Merbach, *J. Magn. Reson.* **1982**, *46*, 319.
[41] A. D. Hugi, L. Helm, A. E. Merbach, *Helv. Chim. Acta* **1985**, *68*, 508.
[42] R. V. Vold, J. S. Waugh, M. P. Klein, D. E. Phelps, *J. Chem. Phys.* **1968**, *48*, 3831.
[43] S. Meiboom, D. Gill, *Rev. Sci. Instrum.* **1958**, *29*, 688.
[44] F. Yerly, VISUALISEUR 2.2.4, Institute of Inorganic and Analytical Chemistry, University of Lausanne (Switzerland), **1999**.
[45] F. Yerly, OPTIMISEUR 2.2.4, Institute of Inorganic and Analytical Chemistry, University of Lausanne (Switzerland), **1999**.
[46] J. Reuben, *J. Chem. Phys.* **1971**, *75*, 3164.
[47] A. Abraham, *The Principles of Nuclear Magnetism*, Oxford University Press, London, **1961**, p. 289.
[48] T. J. Swift, R. E. Connick, *J. Chem. Phys.* **1962**, *37*, 307.
[49] J. R. Zimmermann, W. E. Brittin, *J. Phys. Chem.* **1957**, *61*, 1328.
[50] H. G. Brittain, J. F Desreux, *Inorg. Chem.* **1984**, *23*, 4459.
[51] G. Gonzalez, H. D. Powell, V. Tissières, A. E. Merbach, *J. Phys. Chem.* **1994**, *98*, 53.
[52] Z. Luz, S. Meiboom, *J. Chem. Phys.* **1964**, *40*, 2686.
[53] J. H. Freed, *J. Chem. Phys.* **1978**, *68*, 4034.
[54] S. H. Koenig, R. D. Brown III, *Prog. Nucl. Magn. Reson. Spectrosc.* **1991**, *22*, 487.

Received: September 6, 2001 [F3535]

  0947-6539/02/0805-1048 $ 17.50+.50/0